Optical Review (2018) 25:181–189
https://doi.org/10.1007/s10043-017-0402-3

REGULAR PAPER

Evaluation of the robustness of estimating five components from a skin spectral image

Rina Akaho[1] · **Misa Hirose**[1] · **Norimichi Tsumura**[1]

Received: 17 May 2017 / Accepted: 22 December 2017 / Published online: 3 February 2018

Abstract
We evaluated the robustness of a method used to estimate five components (i.e., melanin, oxy-hemoglobin, deoxy-hemoglobin, shading, and surface reflectance) from the spectral reflectance of skin at five wavelengths against noise and a change in epidermis thickness. We also estimated the five components from recorded images of age spots and circles under the eyes using the method. We found that noise in the image must be no more 0.1% to accurately estimate the five components and that the thickness of the epidermis affects the estimation. We acquired the distribution of major causes for age spots and circles under the eyes by applying the method to recorded spectral images.

Keywords Spectral · Skin · Melanin · Hemoglobin · Oxygen saturation · Monte Carlo simulation

1 Introduction

Skin is a three-layered tissue composed of epidermis, dermis, and subcutaneous tissues, and has chromophores, such as melanin, oxy-hemoglobin, and deoxy-hemoglobin. The reflectance of human skin depends on the thickness of layers, the concentrations of chromophores, and the shapes of parts. Only the concentrations of three chromophores are mainly related to evaluation in cosmetic field like age spot and dark circles under the eyes.

The analysis of diffuse reflectance provides information on tissue activities related to chromophores. This information can be applied to the early detection of skin disease and the monitoring of health. Methods of estimating four components: melanin; blood volume; oxygen saturation; shading (other than surface reflection) have been proposed as follows. Concentrations of chromophores can be treated as parameters and components of the skin structure can be treated as constant as in the previous research. Tsumura et al. discussed a method of determining melanin and hemoglobin concentrations by applying independent component analysis to a skin color image [1]. Kikuchi et al. proposed a method of obtaining the hemoglobin oxygen saturation ratio in the face via multiple regression analysis of images recorded with a spectral camera [2]. Many studies have applied these methods to estimate the four components (other than surface reflection) linearly from skin color images and spectral images. Meanwhile, Kobayashi et al. analyzed the nonlinear relationship between the absorbance and chromophore concentration of skin by conducting Monte Carlo simulation and using the modified Lambert Beer's law, and reported a method of estimating the optical path length for each layer from the absorbance and the concentration of chromophores and shading [3]. However, this method cannot estimate the optical path length if the concentration of chromophores is not given. Even if the concentration is known, the estimation accuracy is insufficient, because the concentration is derived linearly by multiple regression analysis. Hirose et al., therefore, proposed a new nonlinear method of estimating three unknown chromophore concentrations, shading, and surface reflection from the spectral reflectance of skin at five wavelengths [4]. The geometric angle and uniformity of the illumination intensity are compensated for by estimating shading and surface reflectance. In reality, however, noise is observed by the effect of the imaging device and the thickness of the epidermis depends on the skin position. In terms of practical use, it is necessary to evaluate the robustness of

A part of this paper was presented at CIC24, held in San Diego, CA, USA.

✉ Rina Akaho
akasanmail.com@gmail.com

[1] Graduate School of Advanced Integration Science, Chiba University, 1-33 Yayoi-cho, Chiba 263-8522, Japan

the method against noise and a change in thickness of the epidermis.

The present paper, therefore, conducts a Monte Carlo simulation to evaluate the robustness of the method used to estimate the five components against noise and a change in epidermis thickness. We also estimate five components from recorded five-band images. Images of age spots and circles under the eyes are captured and analyzed.

2 Method of estimating the five components

2.1 Analysis of the relationship between absorbance and chromophore concentration

Hirose et al. analyzed the relation between the absorbance and chromophore concentration by conducting a Monte Carlo simulation [4]. We first obtain diffuse reflectance data for skin by the Monte Carlo simulation of light transport in multi-layered tissue (MCML), as proposed by Jacques et al. [5]. MCML is accomplished by following the propagation of photons in tissue. As shown in Fig. 1, we assumed a two-layered skin model composed of the epidermis and dermis. Five optical parameters, namely thickness t, reflective index n, anisotropy factor g, scattering coefficient μ_s, and absorption coefficient μ_a, are set in each layer. The thicknesses t of the epidermis and dermis are 0.006 and 0.40 cm, respectively, in this work. The reflective index n, scattering coefficient μ_s, and anisotropy factor g of the two layers have the same values; $n = 1.4$, while μ_s and g are shown in Fig. 2 [6]. The absorption coefficient μ_a is calculated from the absorption coefficients of chromophores, namely melanin, oxy-hemoglobin, and deoxy-hemoglobin, as follows:

$$\begin{aligned}\mu_{\mathrm{a.epi}}(\lambda) &= \mathrm{Mel} \times \mu_{\mathrm{a.mel}}(\lambda),\\ \mu_{\mathrm{a.der}}(\lambda) &= \mathrm{Ohb} \times \mu_{\mathrm{a.ohb}}(\lambda) + \mathrm{Hb} \times \mu_{\mathrm{a.hb}}(\lambda)\\ &= \mathrm{Thb} \times \mathrm{StO} \times \mu_{\mathrm{a.ohb}}(\lambda) + \mathrm{Thb} \times (1 - \mathrm{StO}) \times \mu_{\mathrm{a.hb}}(\lambda),\end{aligned} \tag{1}$$

where λ is the wavelength and the subscripts of the absorption coefficient epi, der, mel, ohb, and hb indicate the epidermis, dermis, melanin, oxy-hemoglobin, and deoxy-hemoglobin, respectively. The absorption coefficients of chromophores are shown in Fig. 3 [6]. The percentages of melanin, oxy-hemoglobin, and deoxy-hemoglobin are denoted Mel, Ohb, and Hb, respectively. We input these percentages of chromophores into MCML to acquire the diffuse reflectance of skin, $R_{\mathrm{MCML}}(\lambda)$. The percentages of oxy-hemoglobin and deoxy-hemoglobin are calculated using the blood volume Thb and oxygen saturation StO. The blood volume is defined as the sum of oxy-hemoglobin and deoxy-hemoglobin volumes, Ohb + Hb. The oxygen saturation is the ratio of oxy-hemoglobin in the blood and is expressed as Ohb/(Ohb + Hb). We set Mel = 1, 2, 3, 4, 5, 6, 7, 8, 9, and 10%; Thb = 0.2, 0.4, 0.6, 0.8, and 1.0%; and StO = 0, 20, 40, 60, 80, and 100%; and acquired 300 reflectance spectra data from their combinations.

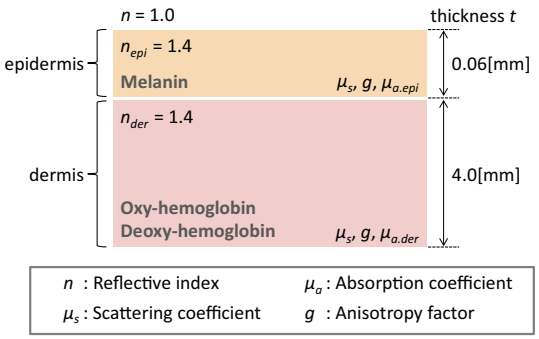

Fig. 1 Two-layered skin model composed of epidermis and dermis

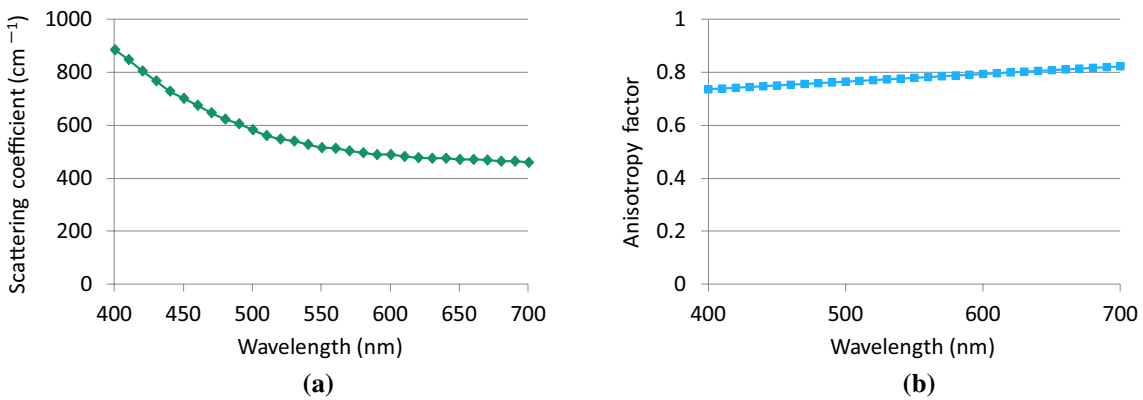

Fig. 2 **a** Scattering coefficient and **b** Anisotropy factor

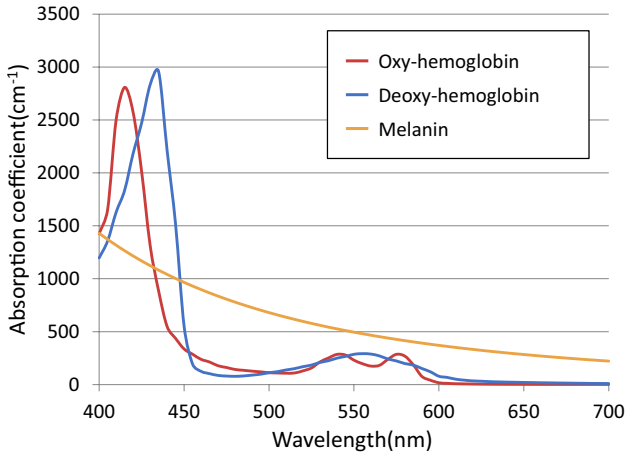

Fig. 3 Absorption coefficient of chromophores, i.e., melanin, oxy-hemoglobin, and deoxy-hemoglobin

Hirose et al. converted the reflectance $R_{\mathrm{MCML}}(\lambda)$ to absorbance $\mathrm{Abs}_{\mathrm{MCML}}(\lambda)$ by taking the negative of the natural logarithm, $-\log(R_{\mathrm{MCML}}(\lambda))$. The relationships between the absorbance at 560, 570, 590, 610, and 700 nm, and chromophore concentration are shown in Fig. 4. These wavelengths are selected from nine wavelengths by optimization [4]. The Z-axis represents the absorbance, while the X-axis and Y-axis indicate the absorption coefficients of the dermis $\mu_{\mathrm{a.der}}(\lambda)$ and the percentage of melanin Mel, respectively. Black dots in Fig. 4 indicate the 300 absorbance spectra $\mathrm{Abs}_{\mathrm{MCML}}(\lambda)$ obtained from MCML. To obtain well-fitting curves for the 300 absorbance data spectra, we model the absorbance Z as a cubic function of X and Y for each wavelength:

$$X + IY + J, \tag{2}$$

where X is $\mu_{\mathrm{a.der}}(\lambda)$, as defined by Eq. (1), and Y is the percentage of melanin Mel. The coefficients A to I and the constant J are determined so as to minimize the residual sum of squares $\mathrm{RSS}_{\mathrm{func}}$ for each wavelength:

$$\mathrm{RSS}_{\mathrm{func}}(\lambda) = \sum_{i=1}^{300} [\mathrm{Abs}_{\mathrm{MCML}}(\lambda, i) - Z(\lambda)]^2, \tag{3}$$

where $\mathrm{Abs}_{\mathrm{MCML}}(i)$ indicates the ith absorbance generated by MCML.

2.2 Estimation of chromophore concentrations, shading, and surface reflectance from five-band images

Hirose et al. proposed the extraction of five components (i.e., melanin, oxy-hemoglobin, deoxy-hemoglobin, shading, and surface reflection) from five-band images of skin using the cubic function $Z(\lambda)$ represented by Eq. (2). It is assumed that the five components can be estimated from the spectral reflectance of skin $R(\lambda)$. Incident light is deflected or absorbed. The light incident on the skin is divided into reflection from the skin surface and diffuse reflection

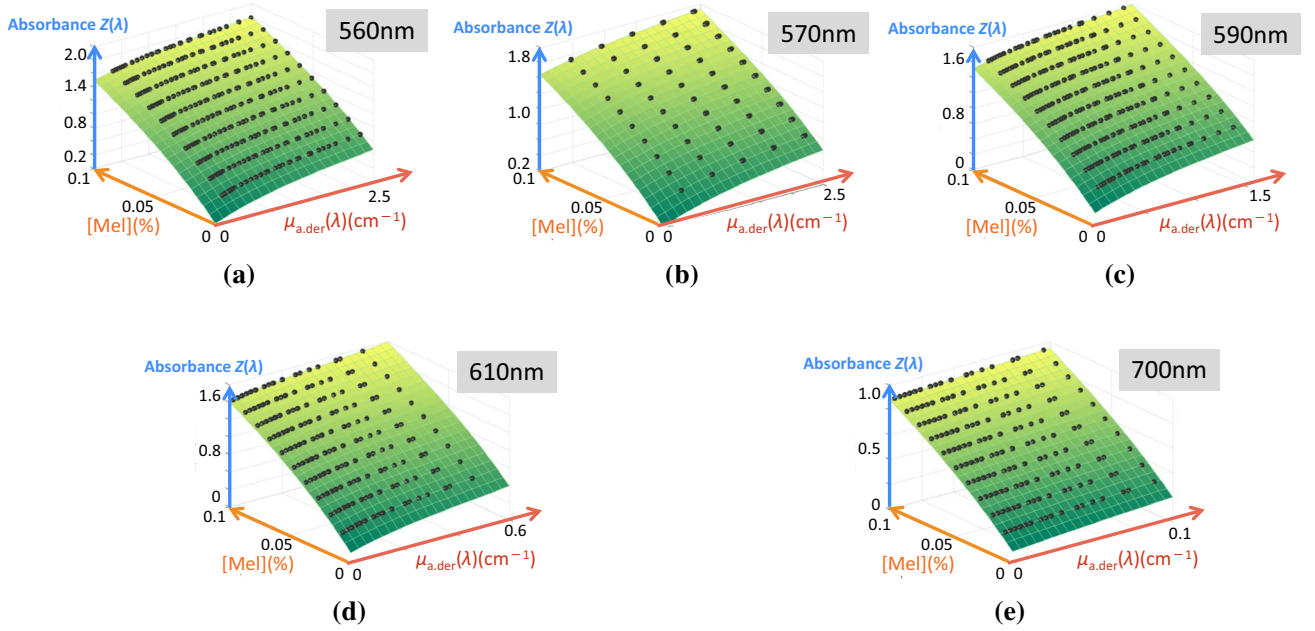

Fig. 4 Nonlinear relationship between Monte Carlo simulation and chromophore concentration at five wavelengths: **a** 560 nm, **b** 570 nm, **c** 590 nm, **d** 610 nm, and **e** 700 nm

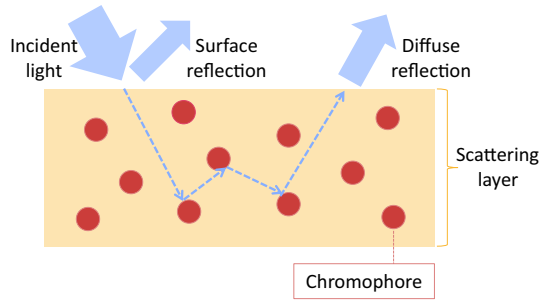

Fig. 5 Reflection properties of the skin

scattered and absorbed by the chromophores, as shown in Fig. 5. The relationship between the diffuse reflection $R_{df}(\lambda)$ and absorption $A(\lambda)$ is as follows:

$$A(\lambda) = -\log(R_{df}(\lambda)). \tag{4}$$

In the case of the Lambert–Beer law, absorbance $A(\lambda)$ can be calculated from the cubic function of absorbance $Z(\lambda)$ and shading k as follows:

$$A(\lambda) = Z(\lambda) + k. \tag{5}$$

The cubic function of absorbance $Z(\lambda)$ is defined in terms of the concentrations of the three chromophores in Eq. (2). Diffuse reflection $R_{df}(\lambda)$ is calculated from Eqs. (4) and (5) as follows:

$$R_{df}(\lambda) = \exp(-(Z(\lambda) + k)). \tag{6}$$

The spectral reflectance of skin $R'(\lambda)$ is, therefore, defined using the surface reflectance R_{sp}:

$$R'(\lambda) = R_{df}(\lambda) + R_{sp} = \exp(-(Z(\lambda) + k)) + R_{sp}. \tag{7}$$

In the presented method, five components are determined so as to minimize the residual sum of squares RSS_{est}, expressed as follows:

$$\mathrm{RSS}_{est} = \sum_{\lambda} [R(\lambda) - \{\exp(-(Z(\lambda) + k)) + R_{sp}\}]^2, \tag{8}$$

and the speed of calculation is about 30 s per pixel.

3 Evaluation of the robustness of the method against noise

Spectral reflectance was simulated by Monte Carlo simulation. We set the melanin concentration Mel = 1, 2, 3, 4, 5, 6, 7, 8, 9, and 10%; blood volume Thb = 0.2, 0.4, 0.6, 0.8, and 1.0%; and oxygen saturation StO = 0, 20, 40, 60, 80, and 100%; and acquired 300 reflectance spectra from their combinations. We added shading and surface reflection to the simulated reflectance. Noise was added to the reflectance map to evaluate the robustness against noise. We used a random number from a uniform distribution multiplied by a constant as the noise. In the case that noise is less than 0.1%, the noise is a uniformly distributed random number between 0 and 0.001 when the reflectance of a white color board is 1. In the case that noise is less than 1.0%, the noise is a uniformly distributed random number between 0 and 0.01. Only noise of three types is added to reflectance in these experiments, to reduce the calculate cost.

The average relative error and the coefficient of correlation between the correct value and the estimated value are shown in Fig. 6. Spectral reflectance data without noise are labeled as "no noise", noise less than 0.1% is labeled "less than 0.1%", and noise less than 1.0% is labeled as "less than 1.0%". In the case that noise is less than 0.1%, the correlation coefficient exceeds 0.8 for all components. However, when noise exceeds 0.1%, the correlation coefficients of the blood volume, shading, and surface reflection are less than 0.6. The accurate estimation of the five components in these

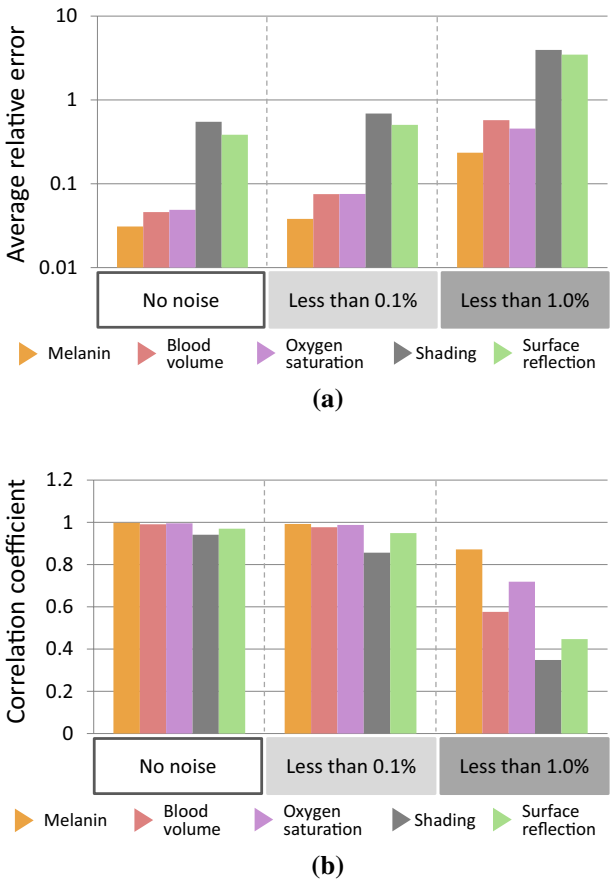

Fig. 6 Average relative error and correlation coefficient between the correct value and the estimated value: **a** average relative error and **b** correlation coefficient. In the case that noise is less than 0.1%, noise is a uniformly distributed random number between 0 and 0.001 when the reflectance of a white color board is 1. In the case that noise is less than 1.0%, the noise is uniformly distributed between 0 and 0.01

experiments, therefore, requires noise in the image to be 0.1% or less.

4 Evaluation of estimation results of the method for varying epidermis thicknesses

The cubic function $Z(\lambda)$ is calculated by Monte Carlo simulation to estimate the five components. The thickness of the epidermis is set as 0.006 cm (i.e., 60 μm). The cubic function $Z(\lambda)$ is, therefore, the absorbance of skin that has an epidermis thickness of 60 μm. However, the thickness of the epidermis varies depending on location, as shown in Table 1 [8]. It is, therefore, necessary to evaluate the estimation results when the epidermis thickness differs from that of the skin model. We generated numerical phantoms with various epidermis thicknesses and evaluated the estimation results.

4.1 Generating a numerical phantom for a spectral reflectance map

Demonstration of the effectiveness of the proposed method requires a numerical phantom, because the chromophore concentration is unknown for actual skin spectral reflectance. We built a numerical phantom by generating a spectral reflectance map with MCML. Figure 7 outlines the generation of a spectral reflectance map.

First, to obtain the distribution of chromophores close to real skin, we extracted the chromophore component by applying independent component analysis to an actual skin color image without surface reflection [1]. We captured this image by setting polarization filters in front of the camera and positioning light sources, so that they were orthogonal to each other. The obtained melanin concentration was divided into three, and the allocated input melanin concentrations of MCML Mel = 3, 6, and 9%. The reason for dividing into three values in melanin components was to reduce the calculation cost. Similarly, the obtained hemoglobin concentration was divided into three, and allocated input blood volume of MCML Thb = 0.2, 0.6, and 1.0%. In addition, we considered two oxygen saturations (StO = 70, 100%) and set the lower oxygen saturation at the center of the map, because oxygen

Table 1 Mean thickness of the epidermis [8]

Body site	Mean thickness (μm)
Palm	429.0
Fingertip	369.0
Back of hand	84.5
Forearm	60.9
Upper arm	43.9
Thoracic region	37.6
Abdomen	46.6
Upper back	43.4
Lower back	43.2
Thigh	54.3
Calf	74.9
Forehead	50.3
Cheek	38.8

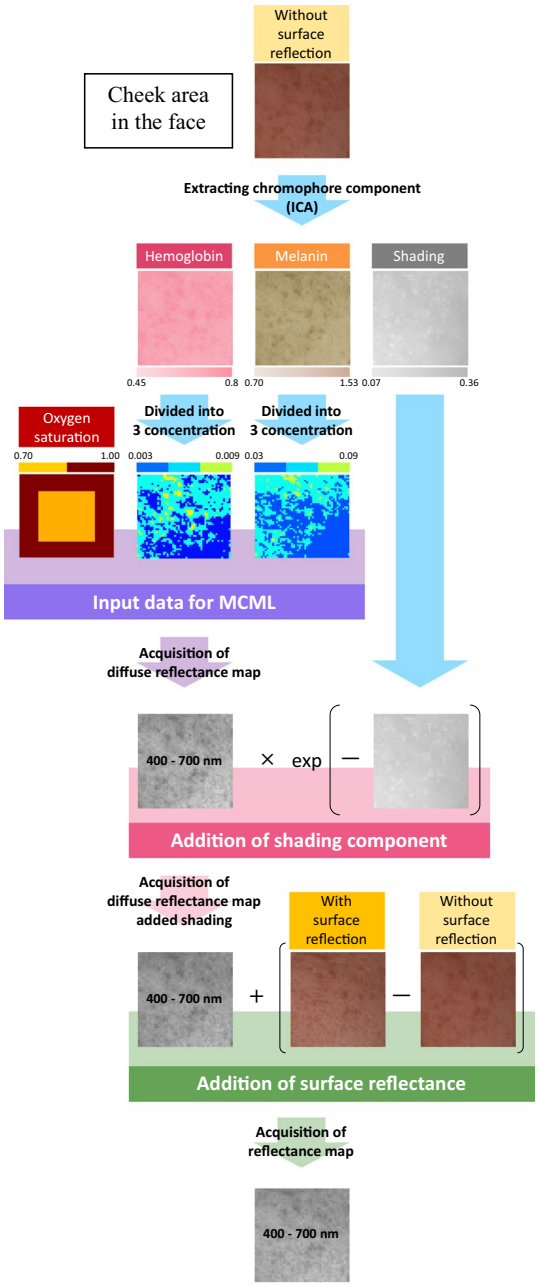

Fig. 7 Outline for generating spectral reflectance map

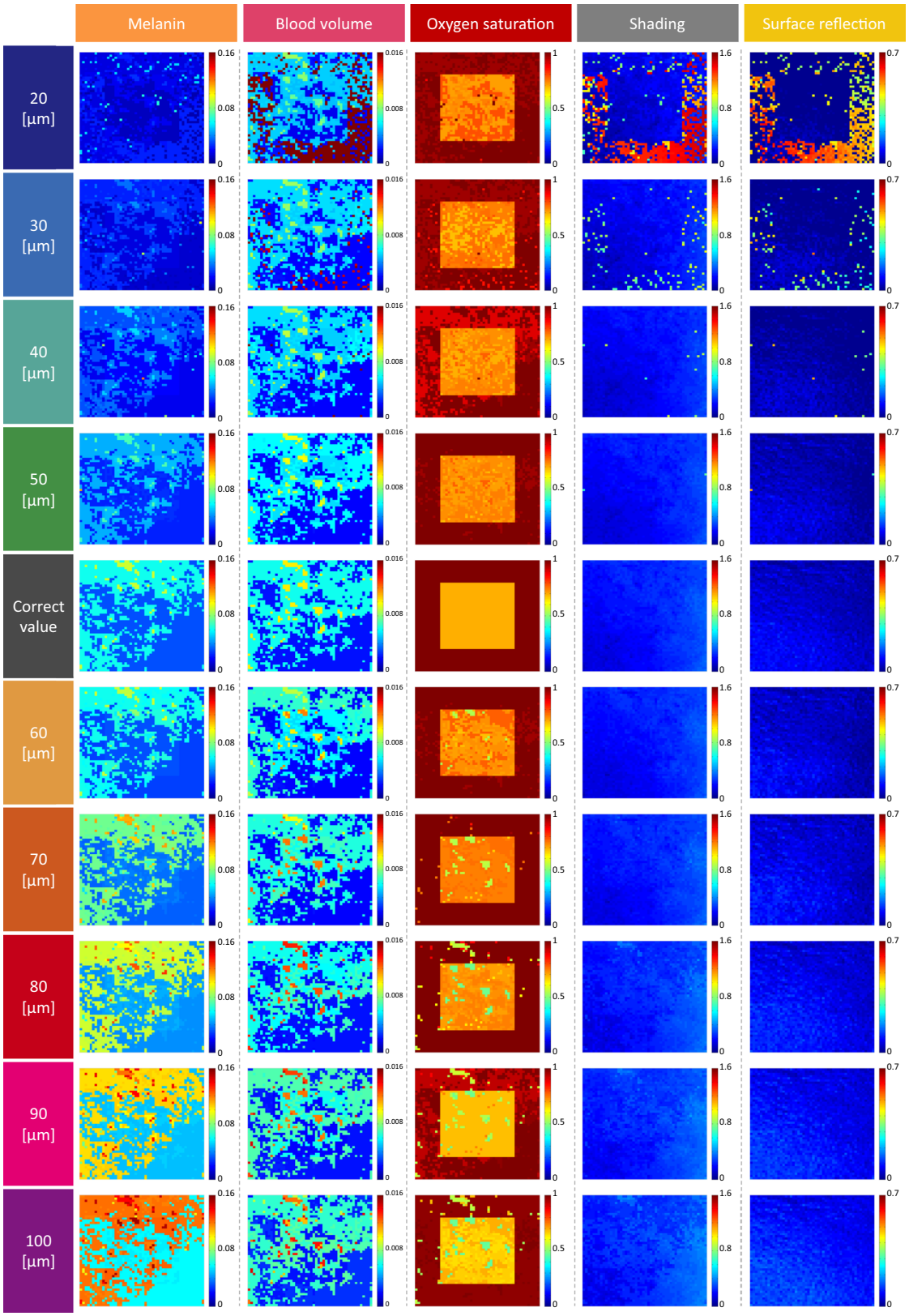

Fig. 8 Concentration distribution of five components when the epidermis thickness is changed

saturation is not acquired using by ICA. This region is intended to represent dark shadows under the eyes. To generate a diffuse reflectance map, we assigned diffuse reflectance from MCML corresponding to the combination of the melanin concentration, blood volume, and oxygen saturation to each pixel.

We next added shading to the diffuse reflectance map to generate images with four components. By adding surface reflectance to this four-component image, we can generate images that have five components. The surface reflectance was calculated from the difference between skin color images with and without surface reflection.

4.2 Evaluating the estimation results of the method for varying epidermis thicknesses

We evaluated the estimation results of our method for varying epidermis thicknesses. Table 1 shows that the epidermis is thicker for the palm and fingertip than for other sites, but ranges 20–100 μm at most sites. The numerical phantom was, therefore, generated with epidermis thicknesses of 20, 30, 40, 50, 60, 70, 80, 90, and 100 μm. Figure 8 shows the five components of the numerical phantom estimated following Sect. 2.2. In the case of a thickness of 60 μm [which is the same thickness as when we calculated the cubic function of absorbance $Z(\lambda)$ for estimation], the distribution and values of estimations are close to the correct distribution and values for all components. When the thickness of the epidermis is decreased highly, the estimated values and estimated distributions are getting apart from the ground truth. With increase the thickness of the epidermis, the estimated values are also getting apart from the ground truth, but estimated distributions are remained to be close to the ground truth. In the blood volume map, shading map, and surface reflection map, the absolute and distribution errors from correct values increase as the difference of the epidermis thickness increases. In the oxygen saturation map, the distribution of oxygen saturation is almost unchanged even if the thickness of the epidermis is changed. However, the estimated values of the oxygen saturation are slightly effected by the values of blood volume.

Therefore, although it is necessary to generate a cubic function $Z(\lambda)$ for each thickness to obtain the absolute value of the concentration, it is necessary to generate a cubic function $Z(\lambda)$ for each thickness if only the trend of map is required.

5 Estimation from a recorded five-band image

5.1 Acquisition of a facial image

Facial images were acquired to estimate the five components from a five-band image using the proposed method. The experimental environment is shown in Fig. 9. The lighting source was a SOLAX XC-500 sun illuminating lamp (SERIC, Tokyo, Japan) and the spectral camera was an ImSpector camera (JFE Techno Research, Tokyo, Japan). Facial images were acquired in a visible region of 400–700 nm. We used information for five wavelengths (i.e., 560, 570, 590, 610, and 700 nm) to estimate the components. Figures 10 and 11 show the recorded images. To evaluate the estimation results, we captured images of age spots and circles under the eyes. Blood congestion is not appeared in these area.

5.2 Estimation results from the recorded five-band image

Figure 12 shows the estimation results obtained using the proposed method from the recorded five-band image of age spots. The cause of an age spot is an increase in melanin only, and it is supposed that the blood volume and oxygen saturation are little changed in an age spot [9]. The melanin concentration is high in the region of the age spot. Except in the region that the value of components is saturated, the blood volume and oxygen saturation are considered to be constant.

Figure 13 shows the estimation results for circles under the eyes. In the figure, the concentration of melanin is high at the top and bottom of a circle under an eye, and shading is seen throughout. In addition, the blood volume

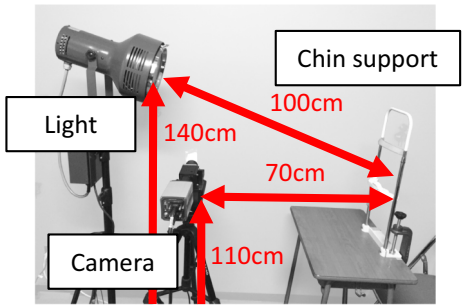

Fig. 9 Experimental environment for acquiring facial image

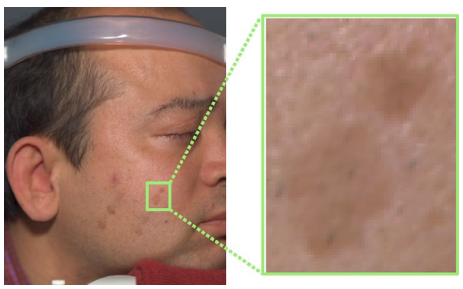

Fig. 10 Image of age spots

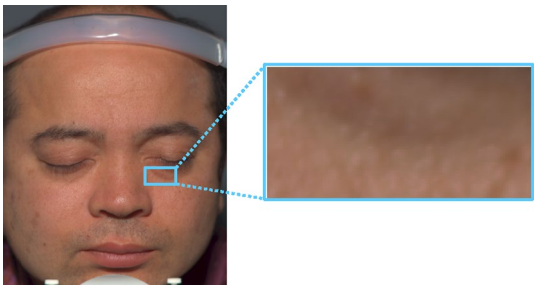

Fig. 11 Image of circle under eyes

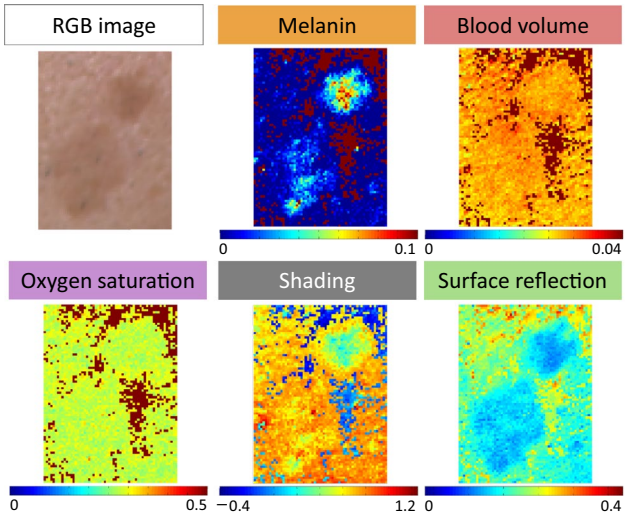

Fig. 12 Estimated concentration distribution of five components from image of age spot

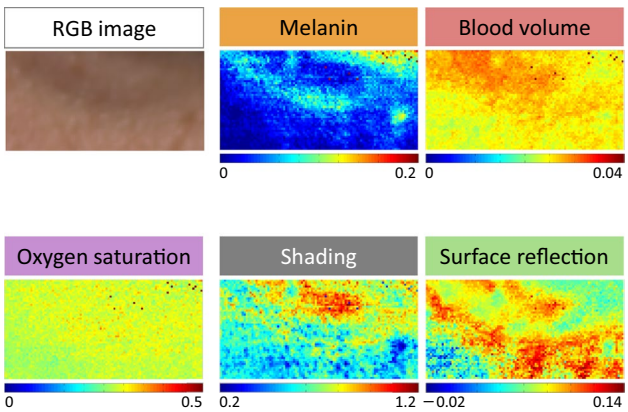

Fig. 13 Estimated concentration distribution of five components from image of circle under eyes

increases toward the inner corner of the eye. This tendency has been demonstrated experimentally [10]. Because oxygen saturation has lower values throughout the image, the concentration of deoxy-hemoglobin is high at the inner corner of the eye. Circles under the eyes are, therefore, attributable to an increase in melanin, in oxy-hemoglobin, and in shading. A comparison of the recorded image and the estimated distribution of surface reflection shows that gloss component has been acquired appropriately from an empirical view point of shape under the eye.

6 Conclusion

We evaluated the robustness of a method used to estimate five components (i.e., melanin, oxy-hemoglobin, deoxy-hemoglobin, shading, and surface reflectance) from the spectral reflectance of skin at five wavelengths with respect to noise and a change in epidermis thickness. We found that the noise of the image must be no more than 0.1% to accurately estimate the five components. The epidermis thickness affects the estimation, but rough distributions of the five components can be obtained. We also estimated the five components from captured images of age spots and circles under the eyes using our method. The distribution of the major causation of age spots and circles under eyes can be acquired by applying our method to recorded images. In the future works, experiments should be performed with ultraviolet irradiation and methyl nicotinate whether it can be estimated correctly for changes in skin components. Furthermore, it is necessary to accelerate the experimental program for practical use. In this research, the estimation model was calculated by using scattering coefficient of fixed value; however, it is necessary to investigate the effect of the scattering coefficients by the layer in the future work.

References

1. Tsumura, N., Ojima, N., Sato, K., et al.: Image-based skin color and texture analysis/synthesis by extracting hemoglobin and melanin information if the skin. ACM Trans. Graph. **22**(3), 770–779 (2003)
2. Kikuchi, K., Masuda, Y., Hirao, T.: Imaging of hemoglobin oxygen saturation ratio in the face by spectral camera and its application to evaluate dark circles. Skin Res. Technol. **19**, 499–507 (2013)
3. Kobayashi, M., Ito, Y., Sakauchi, N., et al.: Analysis of nonlinear relation for skin hemoglobin imaging. Opt. Soc. Am. **9**(13), 802–812 (2001)
4. Hirose, M., Tsumura, N.: Nonlinear estimation of chromophore concentrations, shading and surface reflectance from five band

images. In: Color and imaging conference, Darmstadt, Germany, proceedings, pp. 161–166 (2015)
5. Wang, L., Jacques, S.L.: Monte Carlo modeling of light transport in multi-layered tissues in standard C, University of Texas M. D. Anderson Cancer Center (1992)
6. Tsumura, N., Kawabuchi, M., Haneishi, H., Miyake, Y.: Mapping pigmentation in human skin from multi-channel visible spectrum image by inverse optical scattering technique. J. Imaging Sci. Technol. **45**(5), 444–450 (2000)
7. Oregon Medical Laser Center, Optical Properties Spectra. http://omlc.org/spectra/. Accessed 30 Nov 2017
8. Poirier, G.: Human skin modelling and rendering. Thesis, M.S., University of Waterloo, (2003)
9. Ojima, N., Tsumura, N., Akazaki, S., Hori, K., Miyake, Y.: Application of image-based skin chromophore analysis to cosmetics. J. Imaging Sci. Technol. **48**(3), 222–236 (2004)
10. Matsumoto, M., Kobayashi, N., Hoshina, O., et al.: Study of causal factors of dark circles around the eyes. IFSCC Mag **4**, 281 (2001)